







# A new simultaneous measurement system of wide Q-range small angle neutron scattering combined with polarized Fourier transform infrared spectroscopy

Cite as: Rev. Sci. Instrum. **90**, 093906 (2019); <https://doi.org/10.1063/1.5112054>

Submitted: 02 June 2019 . Accepted: 04 September 2019 . Published Online: 30 September 2019

Fumitoshi Kaneko , Tatsuya Kawaguchi, Aurel Radulescu , Hiroki Iwase , Toshiaki Morikawa, Shin-ichi Takata , Masayoshi Nishiura , and Zhaomin Hou 



View Online



Export Citation



CrossMark

## Lock-in Amplifiers up to 600 MHz

starting at

\$6,210



Zurich  
Instruments

Watch the Video



# A new simultaneous measurement system of wide Q-range small angle neutron scattering combined with polarized Fourier transform infrared spectroscopy

Cite as: Rev. Sci. Instrum. 90, 093906 (2019); doi: 10.1063/1.5112054

Submitted: 2 June 2019 • Accepted: 4 September 2019 •

Published Online: 30 September 2019



Fumitoshi Kaneko,<sup>1,a)</sup> Tatsuya Kawaguchi,<sup>1</sup> Aurel Radulescu,<sup>2</sup> Hiroki Iwase,<sup>3</sup> Toshiaki Morikawa,<sup>3</sup> Shin-ichi Takata,<sup>4</sup> Masayoshi Nishiura,<sup>5</sup> and Zhaomin Hou<sup>5</sup>

## AFFILIATIONS

<sup>1</sup>Graduate School of Science, Osaka University, 1-1 Machikaneyama, Toyonaka, Osaka 560-0043, Japan

<sup>2</sup>Jülich Centre for Neutron Science (JCNS) at Heinz Maier-Leibnitz Zentrum (MLZ), Lichtenbergstr. 1, 85748 Garching, Germany

<sup>3</sup>Neutron Science and Technology Center, Comprehensive Research Organization for Science and Society (CROSS), 162-1 Shirakata, Tokai, Ibaraki 319-1106, Japan

<sup>4</sup>Materials and Life Science Division, J-PARC Center, Tokai, Ibaraki 319-1195, Japan

<sup>5</sup>Organometallic Chemistry Laboratory, RIKEN Cluster for Pioneering Research, Wako, Saitama 351-0198, Japan

<sup>a)</sup>E-mail: toshi@chem.sci.osaka-u.ac.jp. Fax: (+81) 6 6850 5455.

## ABSTRACT

Small angle neutron scattering (SANS) is a versatile and convenient method to investigate the higher order structure of molecular assembly systems. However, the more complicated a system of interest, the more difficult the interpretation in the SANS profile. In order to increase the reliability of structural analysis on a complicated system, it is desirable to obtain different kinds of structural information from the same sample simultaneously. Polarized infrared spectroscopy is able to provide information about the molecular structure, concentration, and orientation of each chemical species in a system. In order to utilize these advantages of polarized infrared spectroscopy, a simultaneous measurement system was built by incorporating a Fourier transform infrared (FTIR) spectrometer into a time-of-flight small angle neutron scattering instrument covering a wide Q range. Using this system, simultaneous measurements of wide- and small-angle neutron scattering and polarized FTIR spectroscopy was realized for the first time.

Published under license by AIP Publishing. <https://doi.org/10.1063/1.5112054>

## I. INTRODUCTION

Small angle neutron scattering (SANS) is a powerful method to investigate the higher order structure of molecular assembly systems<sup>1,2</sup> and has expanded its presence even in the research concerning time-dependent structural evolution. In combination with a partial deuteration technique, SANS is able to characterize a specific part in a complex system. Since its scattering pattern is determined by the scattering length density (SLD) profile, the interpretation in a SANS profile is not so easy for a complex system. On the other hand, vibrational spectroscopy, which is able to provide local molecular level structural information of each component, has been employed

as a complementary tool to diffractometry. In particular, Fourier Transform infrared (FTIR) spectroscopy is a convenient method to follow a time-evolution of the structure in a system. We had developed a simultaneous SANS/FTIR spectroscopy measuring system at a steady-state SANS instrument [KWS-2 diffractometer, Heinz Maier Leibnitz Zentrum (MLZ), Germany]. By using this measuring system, we studied the structure of a syndiotactic polystyrene (sPS) film including various guest molecules.<sup>3,4</sup> We intended to observe higher order crystalline structures by SANS and that local molecular configuration and molecular packing by FTIR. It was showed that the FTIR data were useful for interpreting and analyzing SANS profiles. In the previous studies, however, it was impossible to directly

observe the changes of lattice reflections caused by guest inclusion and obtain detailed information about the structure and orientation of guest molecules.

We expect that the structural information related to guest molecules is reflected in the  $Q$ -range higher than that for SANS and also in the polarization of IR bands. Therefore, we need to extend the measurable  $Q$ -range for wide-angle neutron scattering (WANS). This is seemingly easily achieved by installing an additional high-angle detector. However, since the  $Q$ -resolution of a SANS profile is dominated by the wavelength resolution, it is actually not easy to carry out neutron scattering measurements at high resolution in the high- $Q$  range without losing SANS intensity in a steady-state SANS instrument.

To overcome this problem, we have newly developed a simultaneous SANS/FTIR system on a time-of-flight SANS instrument. The small and wide angle neutron scattering instrument (TAIKAN) installed at the Material and Life Science Experimental Facility (MLF), Japan Proton Accelerator Research Complex (J-PARC) can simultaneously cover a wide- $Q$  range.<sup>5</sup> In the development of this new system, we have totally redesigned the optical system including FTIR spectrometer for easier optical-path adjustment and higher light utilization efficiency. Furthermore, to obtain information about the orientation of constituent molecules, we have introduced a device for the measurement of polarization-dependent infrared absorption. To evaluate the performance of this system, we have carried out temperature dependent measurements on two kinds of sPS cocrystal containing toluene and diethylene glycol dibenzoate (DEGDBA) as guests, respectively. Toluene is a typical and well known guest of sPS and occupies one cavity in the unit cell. On the

other hand, DEGDBA consisting of two aromatic rings and a connecting bridge portion is a newly found guest; it is expected that the two aromatic rings are separately accommodated into two cavities. We are interested in whether polarized IR spectroscopy would provide the information about the orientation of these guest molecules, in particular, of their aromatic rings and whether this new system would clearly differentiate in thermal behavior between sPS/toluene and sPS/DEGDBA cocrystals. In this paper, we will describe the detail of the newly developed system and show the obtained results for temperature dependence of the two kinds of sPS cocrystal films.

## II. INSTRUMENTATION

### A. TOF SANS instrument

The TAIKAN instrument was installed on the BL15 beamline at MLF, J-PARC, Tokai, Japan.<sup>5</sup> More than  $1500\text{ }^3\text{He}$  one-dimensional position sensitive detectors are arranged in the four detector banks: small, middle, high-angle, and backward detector bank. Using large-area detector banks and white neutron beams in the wavelength ( $\lambda$ ) range of  $\lambda \sim 0.7\text{--}8\text{ \AA}$  together with the TOF method, TAIKAN can simultaneously cover a  $Q$ -range from  $5 \times 10^{-3}$  to  $15\text{ \AA}^{-1}$ . Using a high-resolution position sensitive scintillation detector, the accessible lower  $Q$ -value achieved the order of  $10^{-4}\text{ \AA}^{-1}$ .

### B. Simultaneous SANS/WANS/FTIR measuring system

Figure 1 shows a newly designed measurement system installed at TAIKAN instrument.<sup>5</sup> An optical system adopted in the present

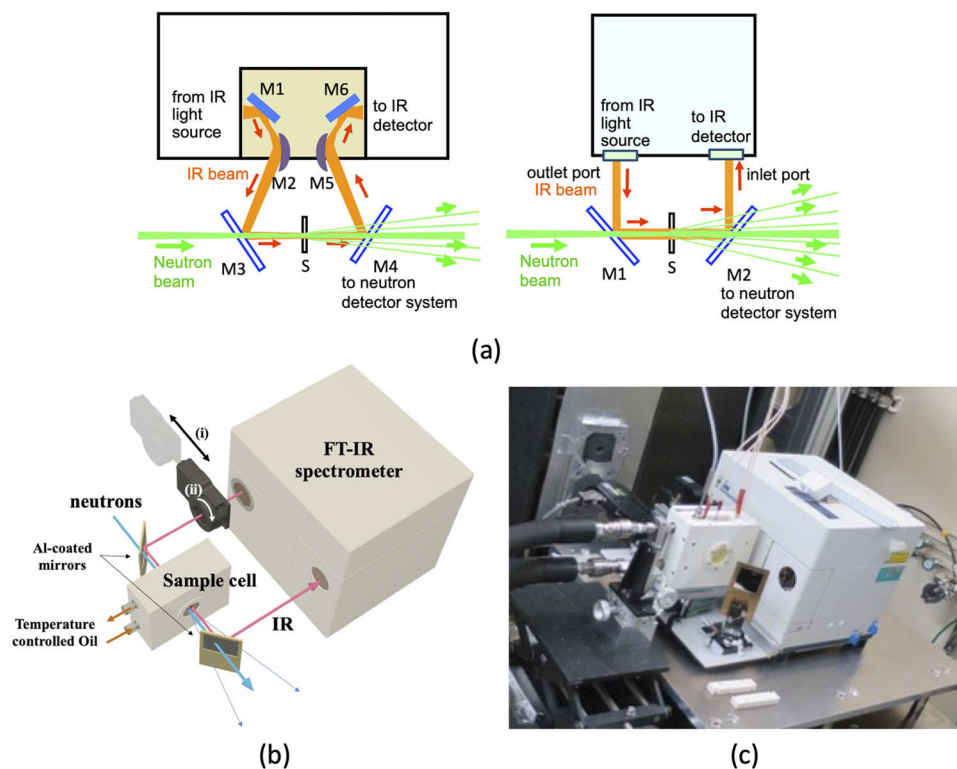


**FIG. 1.** (a) Schematic representation of the arrangements of optical elements for the simultaneous measurement system (left: the previous system and right: the present one). The letter S and the letter M with a digit stand for sample and mirror, respectively. (b) Schematic representation of the polarizer system for polarized FTIR measurements. There is a combination of two remote control stages for translational and rotational movements shown by a straight arrow (i) and a curved arrow (ii), respectively. An IR polarizer is mounted on the rotational stage. The IR polarizer is moved in and out of the IR light path by the translational stage, and its orientation is adjusted by the rotational stage. (c) Actual experimental setup at TAIKAN.

simultaneous measurement system is simpler than that in the previous system,<sup>3,4</sup> which is realized by replacing the FTIR spectrometer. The portable spectrometer used for the previous system (Figure 1a left) is a conventional type equipped with a sample chamber. In order to focus the infrared (IR) beam at the sample position outside the spectrometer, the optical system consists of six mirrors: mirrors 1 and 6 are ordinary flat mirrors, mirrors 2 and 5 are concave mirrors, and mirrors 3 and 4 are Al coated quartz plates with thickness of 0.5 mm that transmit the neutron beam efficiently and reflect only the IR beam. Therefore, mirror 3 acts as a mixer of neutron and IR beams and mirror 4 beam as a separator of them, allowing the two kinds of beams to irradiate the same sample position coaxially.

The renewed FTIR spectrometer (JASCO, VIR-200) of the present system [Fig. 1(a) right] is the one designed for conducting FTIR measurements under a variety of conditions; it has no sample chamber and instead is equipped with two optical ports in the same lateral face; one is an outlet port for emitting parallel light and the other is an inlet port for the incoming light. The optical-port arrangement gives us great flexibility in designing the optical system. As a result, the number of optical mirrors has been remarkably reduced. Only the two Al coated quartz plates are left, which contributes to the benefits of much easier optical-path adjustment and higher light utilization efficiency.

For polarized IR measurements, the current FTIR system is equipped with an IR polarizer unit, which consists of an IR polarizer (KRS-5 wire grid type) and a combination of remote control translational and rotational stages (Sigma Koki Co., Ltd.) [(i) and (ii) in Fig. 1(b)]. During polarized FTIR measurements, the IR polarizer is inserted into the optical path just after the outlet port and its orientation is adjusted, both of which are remotely operated through the control software system for TAIKAN instrument.

### III. EXPERIMENTAL SECTION

#### A. Samples

As demonstration for this measurement system, sPS cocrystal films<sup>6</sup> were prepared by the following procedure.<sup>7</sup> Fully deuterated sPS (d-sPS) (weight average molecular weight:  $2.3 \times 10^5$ ) was synthesized through the coordination polymerization using a rare earth catalyst from fully deuterated styrene with an isotopic purity of 98%.<sup>8</sup> Uniaxially oriented amorphous d-sPS films, about 50  $\mu\text{m}$  thick, were prepared by quenching a melt of d-sPS in an ice-water bath, drawing the melt-quenched film four times at 373 K and clipping well oriented portions from the drawn films. d-sPS cocrystal films containing toluene as guest (d-sPS/h-toluene) were obtained by exposing the oriented amorphous films to a vapor of toluene. To obtain d-sPS cocrystal containing DEGDBA (d-sPS/h-DEGDBA), some of the d-sPS/h-toluene films were subjected to the plasticizer assisted guest exchange procedure. These films were kept in a vacuum drier at 40 °C for 1 h before measurements.

#### B. Simultaneous SANS/WANS/FTIR measurement

We installed the FTIR system with the two mirrors and the IR polarizer unit at the sample position of TAIKAN. The sample cell was set between two mirrors. Figure 1(c) shows a photograph of the FTIR system installed on TAIKAN. The measured sample area was a circle with a diameter of 10 mm. The temperature of the

sample cell was controlled within the accuracy of  $\pm 0.5$  °C by circulating thermostated oil. Transmission IR measurements were carried out at a resolution of 4  $\text{cm}^{-1}$  and at about 5 min interval with a D-TGS detector. Polarized spectra in the range of 4000–400  $\text{cm}^{-1}$  were taken with IR radiation polarized parallel and perpendicular to the drawing direction.

### IV. RESULTS AND DISCUSSION

Figures 2(a) and 2(b) show temperature dependence of two-dimensional (2D) scattering profiles measured on TAIKAN. The drawing direction of the sPS cocrystal sample is shown by a white arrow, and therefore, the equator and ordinates are parallel to the x and y axis of Figs. 2(a) and 2(b). The distribution of protonated guest molecules in the d-sPS cocrystal film is reflected sensitively in the 2D profile, especially in the lamellar reflections appearing on the meridian of the SANS region ( $Q_y = 0.063 \text{ \AA}^{-1}$ ) and the 010 reflections appearing on the equator of the high Q region (around  $Q_x = 0.58 \text{ \AA}^{-1}$ ), respectively.

The lamellar reflections are caused by the scattering length density (SLD) contrast between the amorphous and crystalline regions of sPS cocrystals. Accordingly, the appearance is not necessarily related to the presence of guest molecules in the crystalline region. Not only a higher guest concentration in the crystal lamellae but also a higher guest concentration in the amorphous region gives rise to the lamellar reflections. On the other hand, the 010 reflections are directly related to the cocrystal structure.<sup>9,10</sup> It corresponds to the repeat distance between polymer sheets that sandwich guest molecules [Fig. 2(c)]. If protonated guest molecules are stored in the lattice, the SLD contrast between polymer sheets and guest arrays increases, leading to the appearance of the 010 reflections.

As shown in Figs. 2(a) and 2(b), both d-sPS/toluene and d-sPS/DEGDBA cocrystals show the 010 reflections at 25 °C, but the reflections gradually wane as the temperature increases, which demonstrates that the crystalline region of d-sPS certainly contains the guest molecules at 25 °C and gradually releases them as the temperature rises in both cocrystal systems. With respect to the lamellar reflections, d-sPS/h-toluene and d-sPS/h-DEGDBA cocrystals show quite different temperature dependence. The lamellar reflections of d-sPS/h-toluene cocrystal gradually decrease as the temperature increases. On the other hand, d-sPS/h-DEGDBA shows no clear lamellar reflections at 25 °C, but they start to appear and increase in intensity on heating. Since the samples employed for this study consist of deuterated sPS matrix and protonated low-mass molecules, the distribution of the latter in the samples determines the SANS profile, as schematically shown in Fig. 2(d), where the solid state of d-sPS cocrystal is depicted as a one-dimensional array of crystalline lamellae (yellow boxes) and interlamellar amorphous regions (white parts). The green circles represent guest molecules. The blue rectangle wave below represents the variation of scattering length density between the crystalline and amorphous regions.

The SANS profile at room temperature is considered to reflect the characteristics of each guest compound. Since the molecular weights of toluene and DEGDBA are 92.1 and 314.3, respectively, toluene is much more volatile than DEGDBA. Therefore, toluene tends to dissipate to the air from the amorphous region of d-sPS cocrystal films and DEGDBA tends to remain there. It can be



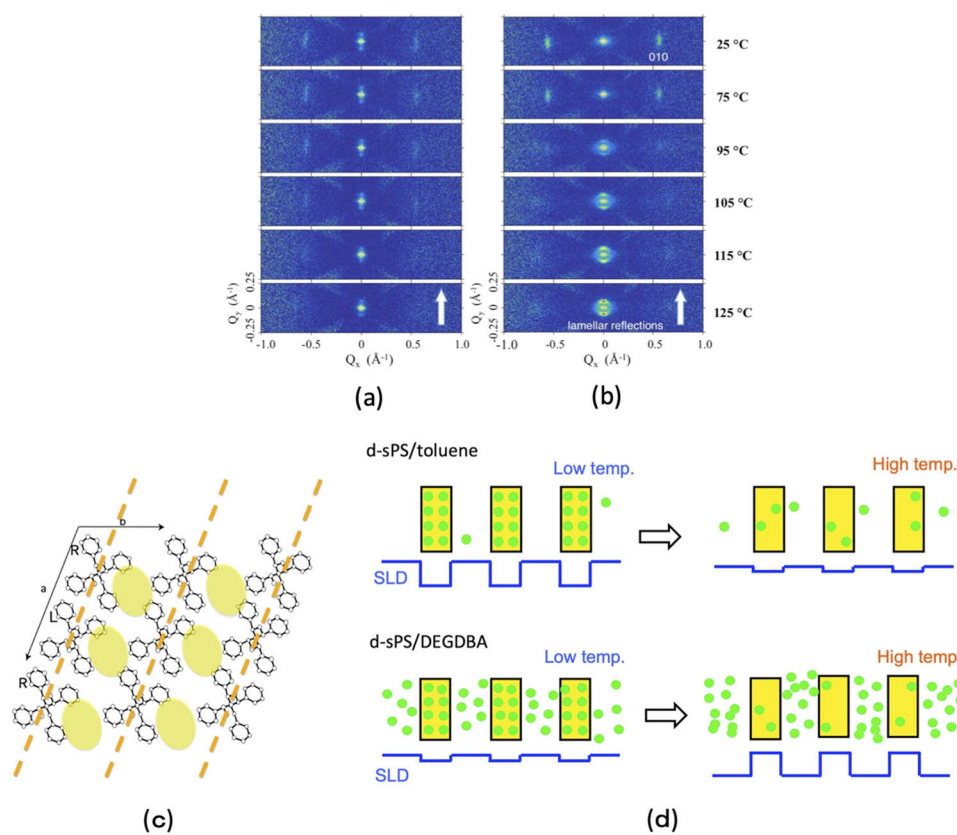


**FIG. 2.** (a) Temperature dependence of neutron scattering profiles observed in d-sPS/h-toluene, (b) those observed in d-sPS/h-DEGDBA cocrystals, (c) a schematic drawing of sPS cocystal lattice viewed along sPS helices where the 010 plane and the guest location are drawn with broken lines and gray yellow ellipses, and (d) a schematic drawing of temperature dependent guest distribution changes in d-sPS/toluene and d-sPS/DEGDBA systems. In (c), the drawing direction of the sPS cocystal sample is perpendicular to the  $ac$  plane.

inferred that most toluene molecules are removed from the amorphous region by the vacuum drying process subsequent to the guest exchange procedure whereas a substantial amount of DEGDBA molecules remain in the amorphous region even after the vacuum drying.

Consequently around the room temperature, toluene molecules are mostly located in the crystalline region, whereas DEGDBA molecules are distributed in both the crystalline and amorphous regions. These leads to a high SLD contrast between the crystalline and amorphous regions in d-sPS/h-toluene cocrystal and a low SLD contrast in d-sPS/h-DEGDBA cocrystal, as schematically shown in Fig. 2(d). When released from the crystal lattice at elevated temperatures, only DEGDBA molecules accumulate in the amorphous region because of the low volatility, which results in a high SLD contrast. A similar influence of guest molecular weight was seen in the lamellar reflections of d-sPS/polyethylene glycol dimethyl ether cocrystals in the previous simultaneous SANS/FTIR study.<sup>11</sup> The simultaneous SANS/WANS measurements clearly provide additional information on this matter.

The polarized FTIR spectra measured in parallel shown in Fig. 3 are consistent with the behavior of guest molecules described above. Both toluene and DEGDBA have monosubstituted benzene rings, which results in the appearance of IR bands due to benzene ring C-H stretch modes in  $3100\text{--}3000\text{ cm}^{-1}$ .<sup>12</sup> The methyl group of toluene shows two bands due to antisymmetric stretch modes at about  $2945$  and  $2920\text{ cm}^{-1}$  and a band due to

symmetric stretch mode at about  $2860\text{ cm}^{-1}$ . At  $25\text{ }^{\circ}\text{C}$ , the d-sPS/h-toluene film exhibits clear polarization in this  $3100\text{--}2800$  region, suggesting that toluene molecules are kept oriented in the crystalline region. As the temperature increases, the toluene bands, both the benzene-ring and methyl-group bands, decrease in intensity keeping their polarization, which means that the toluene molecules released from the lattice dissipate smoothly to the outside and the remaining toluene molecules are still highly oriented in the lattice. Such significant intensity changes are not observed for d-sPS/h-DEGDBA, as shown in as shown in Fig. 3(b). However, there occurs a change in polarization. Although the benzene ring C-H stretch bands in the  $3100\text{--}3000\text{ cm}^{-1}$  region are polarized to some extent at  $25\text{ }^{\circ}\text{C}$ , they show no clear polarization at  $125\text{ }^{\circ}\text{C}$ . Since the polarization in the  $3100\text{--}3000\text{ cm}^{-1}$  region reflects the oriented benzene rings of DEGDBA in the crystalline region just like the guest toluene in d-sPS/h-toluene cocrystal, the temperature dependent changes in IR polarization provide another crucial evidence that the intensity increase of the lamellar reflections at the high temperatures is caused by the migration of h-DEGDBA molecules from the crystalline region into the amorphous region. Two benzoate groups in DEGDBA are linked by a  $\text{C}_2\text{H}_4\text{OC}_2\text{H}_4$  group. The broad absorption around  $2950$  and  $2900\text{ cm}^{-1}$  are assigned to the antisymmetric and symmetric  $\text{CH}_2$  modes of this portion, respectively.<sup>13</sup> It can be inferred that a significant conformational change of the  $\text{C}_2\text{H}_4\text{OC}_2\text{H}_4$  group takes place when DEGDBA molecules migrate from the crystalline region to the amorphous region on heating

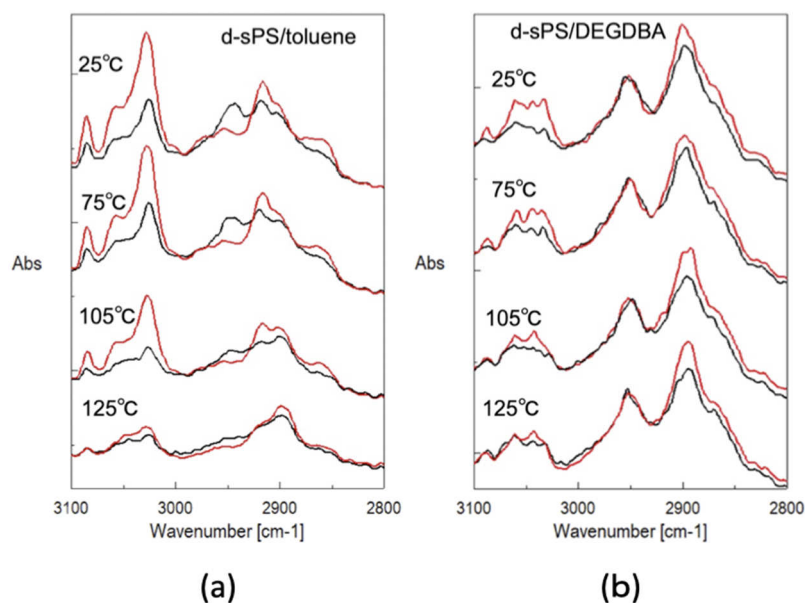


**FIG. 3.** Temperature dependent changes of FTIR spectra measured with polarized radiation parallel (black line) and perpendicular (red line) to the drawing direction; (a) d-sPS/h-toluene cocrystal and (b) d-sPS/h-DEGDBA cocrystal.

process. Therefore, the observed temperature dependent changes around  $2900\text{ cm}^{-1}$  are ascribable to the conformational change of this portion, but a more detailed study is required to confirm this supposition.

The IR bands due to host d-sPS exhibit quite different temperature dependence from those due to the guest molecule. There are two kinds of frequency shifts when host sPS is deuterated: vibrational modes where hydrogen atoms are mainly involved show significant lower frequency shifts, e.g., the CH stretch modes appearing in the range of  $3100\text{--}2800\text{ cm}^{-1}$  shift to the region of  $2300\text{--}2000\text{ cm}^{-1}$ , whereas those ascribable mainly to the displacements of carbon atoms do not show any large shifts, e.g., the phenyl ring CC stretch band shifts from  $1600\text{ cm}^{-1}$  to  $1570\text{ cm}^{-1}$ . Irrespective of the extent of frequency shift, the IR bands due to the host d-sPS do not exhibit any marked changes not only in frequency but also in dichroic ratio on heating up to  $125^\circ\text{C}$ , which is a strong contrast to the remarkable spectral changes in the bands due to the guest molecule. This nature of d-sPS bands can be regarded as a reflection of the thermal stability of sPS helices.

A series of solid-state transformations, cocrystal  $\rightarrow \gamma \rightarrow \alpha$ , take place before the  $\alpha$  phase finally fuses at around  $270^\circ\text{C}$ .<sup>14</sup> According to the X-ray scattering studies using drawn sPS samples, the conformation of sPS helices remains unchanged until the transformation of  $\gamma$  to  $\alpha$  around  $200^\circ\text{C}$  and the orientation of the sPS chain maintains up to the fusion of  $\alpha$ .<sup>15</sup> The present observation that host d-sPS does not exhibit distinct IR spectral changes on heating up to  $125^\circ\text{C}$  is consistent with such thermal tolerance of sPS crystalline region.

## V. SUMMARY

We successfully developed a simultaneous measurement system for SANS/WANS and polarized FTIR, which provides different kinds of structural information. Owing to the extension of the Q-range, structural information in a wide range of scales has become available. The hierarchical structures in crystalline polymers are

accessible. Furthermore, we can access the information about the amount and orientation of some chemical species. With the help of the combined information, more reliable structural analysis can be achieved. This simultaneous system has clearly indicated differences in thermal behavior between sPS/toluene and sPS/DEGDBA cocrystals. We believe that the methodology presented here is applicable to a wide range of soft matter systems.

## ACKNOWLEDGMENTS

This work was partially supported by JSPS KAKENHI Grant (No. JP25410014, F. Kaneko) and the International Joint Research Promotion Program of Osaka University. The SANS experiments were performed with the approval of the Neutron Program Review Committee (Proposal Nos. 2016A0198 and 2017B0158).

## REFERENCES

- <sup>1</sup>R. J. Roe, *Methods of X-Ray and Neutron Scattering in Polymer Science* (Oxford University Press, 2000).
- <sup>2</sup>J. S. Higgins and H. Benoit, *Polymers and Neutron Scattering* (Oxford University Press, 1996).
- <sup>3</sup>F. Kaneko, N. Seto, S. Sato, A. Radulescu, M. M. Schiavone, J. Allgaier, and K. Ute, *Chem. Lett.* **44**, 497–499 (2015).
- <sup>4</sup>F. Kaneko, N. Seto, S. Sato, A. Radulescu, M. M. Schiavone, J. Allgaier, and K. Ute, *J. Phys.: Conf. Ser.* **746**, 012065 (2016).
- <sup>5</sup>S. Takata, J. Susuki, T. Shinohara, T. Oku, T. Tominaga, K. Ohishi, H. Iwase, T. Nakatani, Y. Inamura, T. Ito, K. Suzuya, K. Aizawa, M. Arai, T. Otomo, and M. Sugiyama, *JPS Conf. Proc.* **8**, 036020 (2015).
- <sup>6</sup>G. Millano and G. Guerra, *Prog. Mater. Sci.* **54**, 68–88 (2009).
- <sup>7</sup>F. Kaneko, A. Radulescu, and K. Ute, *Polymer* **54**, 3145–3149 (2013).
- <sup>8</sup>M. Nishiura, F. Guo, and Z. Hou, *Acc. Chem. Res.* **48**, 2209–2220 (2015).
- <sup>9</sup>Y. Chatani, Y. Shimane, T. Inagaki, T. Ijitsu, T. Yukinari, and H. Shikuma, *Polymer* **34**, 1620–1624 (1993).
- <sup>10</sup>C. Daniel, A. Menelle, A. Brulet, and J.-M. Guenet, *Polymer* **38**, 4193–4199 (1997).

<sup>11</sup>F. Kaneko, N. Seto, S. Sato, A. Radulescu, M. M. Schiavone, J. Allgaier, and K. Ute, *J. Appl. Crystallogr.* **49**, 1420–1427 (2016).

<sup>12</sup>R. Knaanie, J. Šebek, M. Tsuge, N. Myllys, L. Khriachtchev, M. Räsänen, B. Albee, E. O. Potma, and R. B. Gerber, *J. Phys. Chem. A* **120**, 3380–3389 (2016).

<sup>13</sup>H. Matsuura, T. Miyazawa, and K. Machida, *Spectrochim. Acta A* **29**, 771–779 (1973).

<sup>14</sup>E. B. Gowd, S. Nair, and C. Ramesh, *Macromolecules* **35**, 8509–8514 (2002).

<sup>15</sup>E. B. Gowd, N. Shibayama, and K. Tashiro, *Macromol. Symp.* **242**, 257–261 (2006).